Microwave Imaging of Multiple Conducting Cylinders Using Local Shape Functions

Weng Cho Chew, *Senior Member, IEEE*, and Gregory P. Otto, *Student Member, IEEE*

***Abstract*—A novel technique is presented for microwave imaging of multiple conducting cylinders using local shape functions. In this method, a scattering volume is divided into small subscattering regions and assigned a local shape function amplitude. The reconstructed image is represented by the set of local shape functions that satisfy multiple scattering boundary conditions. Monochromatic image reconstructions have a resolution scale of 0.1 λ for single scatterers; multiple scatterers can be resolved at a separation of 0.42 λ.**

I. Introduction

MUCH work has been done recently on the microwave imaging of conducting cylinders in the resonance region. A previous algorithm for microwave imaging of conducting objects in the resonance region parameterizes the conducting cylinder shape as a function of polar angle [1]. This is done in order to obtain a single-valued function that is eventually optimized as a function of θ. Unfortunately, this method requires each metallic scatterer's approximate center to be known. Hence, this method is not as versatile as say the Born iterative methods [2] for dielectric scatterers. However, the Born iterative methods are not convergent for conducting scatterers.

This letter presents a novel and versatile technique for microwave imaging of multiple metallic cylinders with E_z incident fields. The novelty stems from the definition of local shape functions assigned to discrete subscatterers and satisfying multiple scattering boundary conditions. This method is more versatile for general multiple metallic inverse scattering problems. An optimization is performed on the measured far-fields to iteratively reconstruct the analog local shape functions.

II. Forward Model

A fixed scattering volume V' containing all possible scatterers can be discretized on a regular grid with grid locations $\boldsymbol{r}_i$ for $i = 1, 2, \ldots, N$. Then, for E_z incident waves, cylindrical conducting scatterers in a volume $V \subset V'$ can be approximately decomposed into smaller conducting cylinders

Manuscript received February 27, 1992. This work was supported by the Army Research Office under Contract DAAL03-87-K0006 to the University of Illinois Advanced Construction Technology Center, by the Office of Naval Research under Grant N00014-89-J-1296, and by the National Science Foundation under Contract ECS-85-52891. The computation time was provided by the National Center for Supercomputing Applications (NCSA) at the University of Illinois at Urbana-Champaign through the Cray Inc. Research and Development Grant.

The authors are with the Electromagnetics Laboratory, Department of Electrical and Computer Engineering, University of Illinois, Urbana, IL 61801.

IEEE Log Number 2901476.

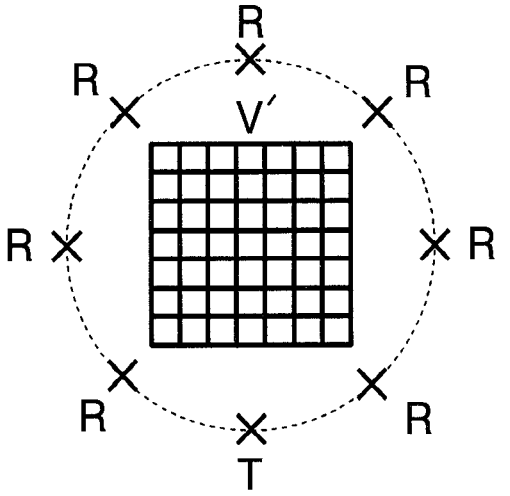

Fig. 1. Data acquisition geometry for microwave imaging measurements. "R" and "T" denote receivers and transmitters, respectively.

(or subscatterers) on this grid, as shown in Fig. 1. Intuitively, this is equivalent to replacing a metallic scatterer with a group of thin wires. In order to represent the discretized scatterers, we assign a binary local *shape function* to each grid location such that

$$\gamma_i = \begin{cases} 1, & \boldsymbol{r}_i \in V, \\ 0, & \boldsymbol{r}_i \notin V. \end{cases} \tag{1}$$

Note that this formulation parameterizes the metallic cylinder's shape in terms of a set of binary local shape functions $\{\gamma_i\}$ with one index i representing grid location.

It is well known that the field from small subscatterers can be expanded in cylindrical harmonics [2]–[4], so that the total field is

$$E_z(\boldsymbol{r}) = \Re g\ \boldsymbol{\psi}^t(k_o, \boldsymbol{r}) \cdot \boldsymbol{e}_o + \sum_{i=1}^{N} \boldsymbol{\psi}^t(k_o, \boldsymbol{r}_i) \cdot\ \boldsymbol{a}_i. \tag{2}$$

where the first term is a multipole expansion in cylindrical harmonics for the incident field in free-space and the second term is a multipole expansion for the scattered field from each subscatterer i.

Finally, the unknown scattering amplitudes $\boldsymbol{a}_i$ can be found by enforcing the boundary conditions on the subscatterers whereby multiple scattering effects are modeled [4]. Notice that the boundary conditions for metallic cylinders are enforced only on subscatterers in scattering volume V, so the T-matrix [2] must be weighted by the local shape function

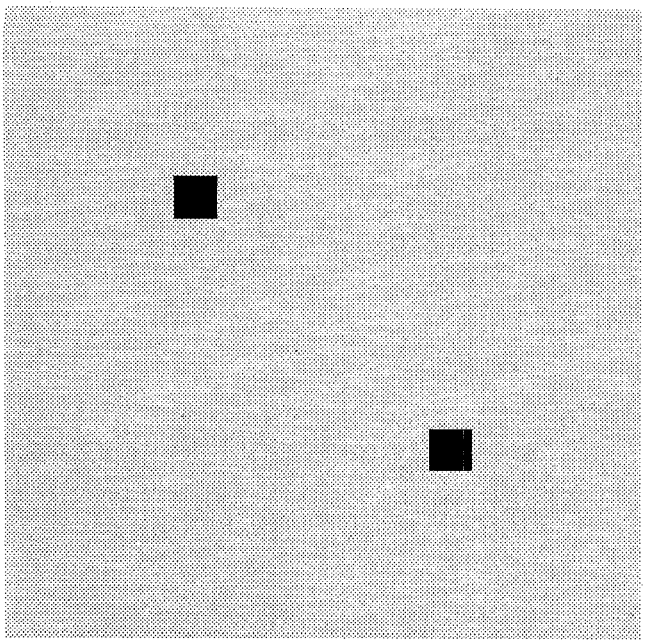

(a)

Fig. 2. (a) True Image of 2 metal cylinders having diameter 0.05 λ and separated by 0.42 λ. Peak value is of 1.0.

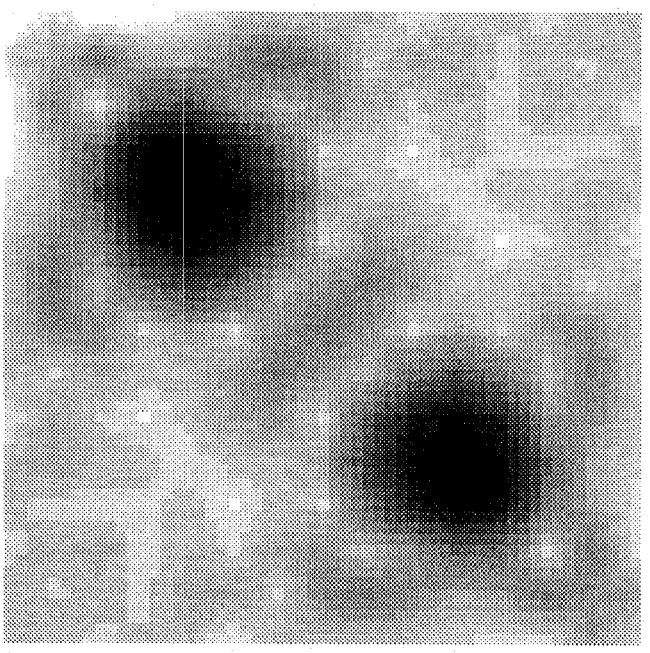

(b)

Fig. 2. (b) Image of 2 metal cylinders having diameter 0.05 λ and separated by 0.42 λ. Reconstruction after 22 iterations with no noise. Peak value is 0.226.

amplitude at each subscatterer. This procedure results in a set of linear equations with a solution given by

$$\boldsymbol{a} = \left[\overline{\mathcal{D}}\,(\boldsymbol{\gamma}) \cdot \overline{\boldsymbol{A}} + \overline{\boldsymbol{I}}\right]^{-1} \cdot \overline{\mathcal{D}}\,(\boldsymbol{\gamma}) \cdot \boldsymbol{b}. \tag{3}$$

Here, the known matrix $\overline{\boldsymbol{A}}$ contains the T-matrices and the translation matrices from other subscatterers to account for multiple scattering interaction. The vector $\boldsymbol{b}$ contains the incident field amplitudes multiplied by the T-matrices. Moreover, the operator $\overline{\mathcal{D}}\,(\boldsymbol{\gamma})$ converts the vector $\boldsymbol{\gamma}$ with elements γ_i to a diagonal matrix. In summary, the forward problem reduces to solving (3) for the harmonic amplitudes of each subscatterer represented by vector $\boldsymbol{a}$, given the local shape functions for each subscatterer in the vector $\boldsymbol{\gamma}$. Then, the field is given by (2).

III. Inverse Model

Basically, the inverse problem is defined as searching through all possible $\boldsymbol{\gamma}$ and choosing the one that minimizes the difference between the measured and computed scattered field. For a set of N binary local shape functions, the number of search directions is 2^N. This is impractical and nonunique since 1) the evanescent fields are not measured and 2) noise is present. Instead, we relax our definition of the local shape functions from binary numbers to complex numbers and we reconstruct the image by minimizing the following linearized cost function at each iteration [5], [6]

$$\min_{\boldsymbol{\gamma}_{k+1}} \left\| \boldsymbol{E}_z^{\text{scat}} - \overline{\boldsymbol{\Psi}}^t \cdot \boldsymbol{a}_k - \overline{\boldsymbol{G}}_k \cdot (\boldsymbol{\gamma}_{k+1} - \boldsymbol{\gamma}_k) \right\|^2 + \delta \left\| \boldsymbol{\gamma}_{k+1} - \boldsymbol{\gamma}_k \right\|^2 \tag{4}$$

where $\boldsymbol{E}_z^{\text{scat}}$ is the measured scattered field and $\overline{\boldsymbol{G}}_k$ is the linearized gradient matrix with respect to $\boldsymbol{\gamma}$ for the forward

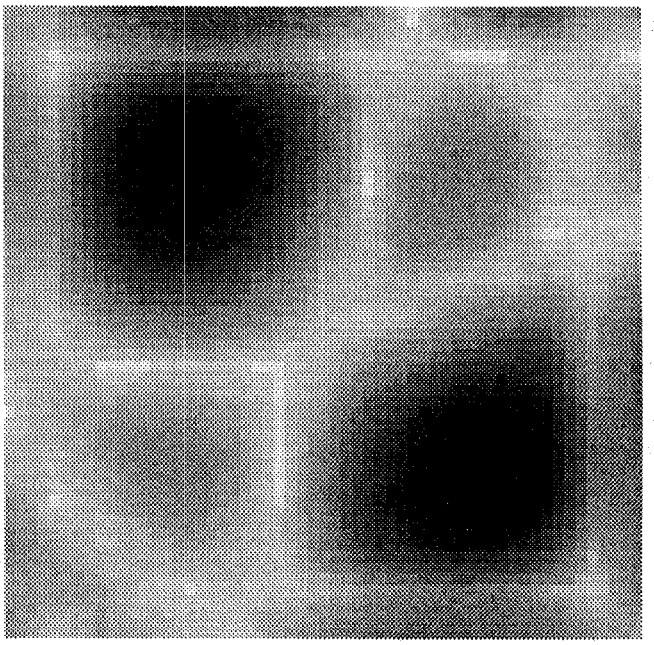

(c)

Fig. 2. (c) Image of 2 metal cylinders having diameter 0.05 λ and separated by 0.42 λ. Reconstruction after 7 iterations with S/N=20 dB. Peak value is 0.094.

problem at iteration $\boldsymbol{\gamma}_k$. The variational solution of the previous minimization problem can be written

$$\boldsymbol{\gamma}_{k+1} = \boldsymbol{\gamma}_k + \left[\overline{\boldsymbol{G}}_k^{\dagger} \cdot \overline{\boldsymbol{G}}_k + \delta \overline{\boldsymbol{I}}\right]^{-1} \overline{\boldsymbol{G}}_k^{\dagger} \cdot \left(\boldsymbol{E}_z^{\text{scat}} - \overline{\boldsymbol{\Psi}}^t \cdot \boldsymbol{a}_k\right). \tag{5}$$

This defines our iterative reconstruction where δ is a small regularization parameter. In this inverse problem, we have allowed the set of local shape functions be a subset of the

complex numbers because of the complex iterative algorithm described by (5). More specifically, the application of the real operator to a set of complex measured fields is not an analytic function and would thereby hinder the convergence of the algorithm.

IV. Results

The gray level plots represent the magnitude of the local shape functions on a 0.05-λ grid with a three point linear interpolation scheme for post-processing. All calculations had a maximum complex phase of 25 degrees for appreciable γ_i. The initial guess for γ_0 is the zero vector. In addition, the choice of regularization parameters is crucial to the convergence of this algorithm. The measured data in this letter are simulated full-angle scattering measurements with 8 transmitters and 36 receivers at a radius of one wavelength, as shown in Fig. 1.

Fig. 2(a) shows the true image of two metal cylinders having diameter 0.05 λ and separated by 0.42 λ. The image reconstruction in Fig. 2(b) has a total size of 0.75-λ square and super-resolution is achieved to a scale of 0.1 λ for each conducting cylinder and 0.42 λ for separating multiple cylinders. Although the peak value of this image is only 0.226, the image becomes sharper and the peak approaches unity as the number of incident angles is increased. Hence, this imaging method is useful for locating conducting cylinders in the resonance region. Finally random gaussian noise was added to the measured data. The image in Fig. 2(c) was reconstructed from data with a signal-to-noise ratio (S/N) of 20 dB, so the image is blurred out and the peak value is decreased to 0.094. One observes that the peak value decreases in these reconstructions because the shape function is more spread out in space. Roughly speaking, the volume of the shape functions is preserved. In order to have the same total scattering strength as a sharp image, a blurred image must have a decreased magnitude.

References

[1] D. Colton and P. Monk, "A novel method for solving the inverse scattering problem for time-harmonic acoustic waves in the resonance region II," *SIAM J. Appl. Math.*, vol. 46, pp. 506–523, 1986.

[2] W. C. Chew, *Waves and Fields in Inhomogeneous Media.* New York: Van Nostrand Reinhold, 1990, pp. 548–557.

[3] W. C. Chew, "An N^2 algorithm for the multiple scattering solution of N scatterers," *Micro. Opt. Tech. Lett.*, vol. 2, pp. 380–383, 1989.

[4] W. C. Chew, L. Gürel, Y. M. Wang, G. Otto, R. L. Wagner, and Q. H. Liu, "A generalized recursive algorithm for wave-scattering solutions in two dimensions," *IEEE Trans. Microwave Theory Tech.*, vol. 40, pp. 716–723, 1992.

[5] Y. M. Wang and W. C. Chew, "An iterative solution of the two-dimensional electromagnetic inverse scattering problem," *Int. J. Imaging Syst. Tech.*, vol. 1, pp. 100–108, 1989.

[6] W. C. Chew and Y. M. Wang, "Reconstruction of two-dimensional permittivity distribution using the distorted Born iterative method," *IEEE Trans. Med. Imaging*, vol. 9, pp. 218–225, 1990.